www.czasopisma.pan.pl PAN www.journals.pan.pl

ARCHIVES of FOUNDRY ENGINEERING

ISSN (2299-2944)
Volume 18
Issue 3/2018

65 – 70

DOI: 10.24425/123603

11/3

Published quarterly as the organ of the Foundry Commission of the Polish Academy of Sciences

Numerical Calculations of the Cast Solidification with the Complex Shape Including the Movement of the Liquid Phase

E. Gawrońska *, R. Dyja
Czestochowa University of Technology,
Dabrowskiego 69, 42-201 Czestochowa, Poland
* Corresponding author. E-mail address: gawronska@icis.pcz.pl

Received 28.05.2018; accepted in revised form 11.07.2018

Abstract

The paper presents the results of the computer simulations of solidification with consideration of the liquid phase movement. Simulations were conducted in a real, complex cast. There is a multi-stage resolution to the problem of convection in solidification simulations. The most important resolution concerns the development of the numerical model with the momentum and continuity equations, as well as conditions which are determined by the convection. Simulations were carried out with the use of our authorial software based on stabilized finite elements method (Petroy-Galerkin). In order to solve Navier-Stokes equation (with the convection element), Boussinesq's approximation were used. Finite Elements Method (FEM) was responsible for the solidification. FEM is close to the heat conduction equation solution (with the internal heat source responsible for the heat released during phase transformation). Convection causes movement in the liquid phase in the solidifying cast and can significantly influence the process of heat transfer from the cast. It may change the distribution of the defects. Results of this article make it possible to assess the conditions in which the influence of the convection on solidification is significant.

Keywords: Solidification, Navier-Stokes, Streamline Upwind Petrov-Galerkin, Pressure Stabilized Petrov-Galerkin

1. Introduction

Solidification remains one of the most troublesome phenomena in numerical modelling. The number and variety of physical processes that take place between microscale and macroscale poses a great challenge to the scientists working on a suitable calculation model connected with diffusion and convection. A great many different models have been proposed over the years that offered reasonable results [1, 2], but they did settle on certain simplifications. None of the results included all of the problems occurring during modelling of this complicated phenomenon.

Many of the calculation models are subject to some restrictions. For instance, one such restriction is the omission of convection force in liquid metal. Unfortunately, their omission in a numerical model may cause crucial differences between the temperature range achieved in a computer simulations, and the temperature of the real casting itself. What is more, due to such a simplification (omission of convection) it is not possible to model certain phenomena which are vital factors influencing the quality

of castings – for example, dopant distribution in the casting or shrinkage during solidification [3].

On the other hand, increasing complexity of models, by including a bigger number of processes (occurring during the solidification) in them, causes problems with the implementation of the models. That is why modern models must be implemented with the use of technology such as parallel computers [4], accelerated architectures, for example GPU (Graphics Processing Unit) [5], or by using specific organization of calculations [6].

In the paper, a solution to the problem of convection in computer simulations of solidification is presented. The paper discusses each stage of the numerical model development, problems connected with occurrence of momentum and continuity equations, as well as conditions in which convection is the key factor. All of that is supplemented with illustrations of the range of temperature, pressure and velocity in different moments of process lasting.

2. Mathematical model

The governing equation for modeling solidification process is based on heat transfer equation with source term:

$$\rho c\dot{T} + \rho c(\mathbf{u}\cdot\nabla)T = \lambda\nabla^2 T + \dot{q}, \tag{1}$$

where T is temperature, $\mathbf{u}$ is velocity from convection force, λ is thermal conductivity, ρ is density, c is specific heat and q is heat source along with the heat of solidification.

In the model solving equation (1) the Newton boundary condition on the external sides of the mould was implemented (heat exchange between the mould and the environment) and the contact condition for the heat exchange between the mould and the casting. Apparent heat capacity formulation can be obtained by using the following form of equation (1):

$$c^*\dot{T} + \rho c(\mathbf{u}\cdot\nabla)T = \lambda\nabla^2 T, \tag{2}$$

where c^* is the approximation of the effective heat capacity. There are different methods to obtain this approximation. Here, the Morgan method is used:

$$c^* = \frac{H^t - H^{t-1}}{T^t - T^{t-1}}, \tag{3}$$

where H is enthalpy and t in superscript is time level.

Liquid metal in this model is assumed to be Newtonian fluid which makes it possible to write Navier-Stokes set of equations as:

$$\rho\dot{\mathbf{u}} + \rho\big((\mathbf{u}\cdot\nabla)\mathbf{u}\big) - \nabla p + \rho\mu\big((\nabla\mathbf{u}) + (\nabla\mathbf{u})^T\big) + \\ + \rho\mu\frac{f_l}{K_\varepsilon}\mathbf{u} = \rho\mathbf{f} \tag{4}$$

$$\nabla\cdot\mathbf{u} = 0, \tag{5}$$

where p is pressure, μ is viscosity, f_l is a liquid fraction, and K_ε is the permeability of the mushy zone.

Above equations are supplemented by the proper set of initial and boundary conditions. Initial $\mathbf{u}$ is set as an initial condition and the no-slip condition is used between the mould and the casting.

The right-hand side of equation (4) describes body forces which arose in liquid. The first part is related to buoyancy force approximated by Boussinesq formula:

$$\mathbf{f} = -\beta\mathbf{g}(T - T_0), \tag{6}$$

where $\boldsymbol{g}$ is gravitational acceleration, β is expansion coefficient, T_0 is reference temperature, which in this particular case is from initial conditions temperature.

The last part of the left-hand side of equation (4) is drag force which appears in a mushy zone due to liquid and an already solidified metal interacting with each other. This model assumes that the solidified part is immovable [7]. The Kozeny-Carman equation approximates the permeability of the mushy zone:

$$K_\varepsilon = K_0\frac{f_l^3}{(1-f_l)^2}, \tag{7}$$

where K_0 is secondary dendrite arm spacing, and f_l is a liquid fraction.

Following simple relation connects liquid fraction with solid fraction:

$$f_l = 1 - f_s, \tag{8}$$

where a value of f_s is taken from phase equilibrium graph relationship:

$$f_s = \frac{1}{1-k}\frac{T_L - T}{T_M - T_L}, \tag{9}$$

where T_L is liquidus temperature, T_M is solidification temperature of the pure component, and k is dopant contribution coefficient.

Equations (1), (4) and (5) are discretised using Finite Element Method, which results in the following set of equations:

$$\mathbf{M}^S\mathbf{T} + (\mathbf{N}^S\mathbf{T} + \mathbf{K}^S)\mathbf{T} = 0 \tag{10}$$

$$\mathbf{M}\mathbf{u} + (\mathbf{N} + \mathbf{K})\mathbf{u} - \mathbf{G}\mathbf{p} + \mathbf{D}\mathbf{u} = \mathbf{F} \tag{11}$$

$$\mathbf{G}^T\mathbf{u} = 0, \tag{12}$$

where superscript S is used to set apart matrices used in solidification equation, and $\mathbf{T}$, $\mathbf{u}$, $\mathbf{p}$ are vectors of unknown temperature, velocity and pressure. Elements of matrices $\mathbf{M}^s$, $\mathbf{M}$, $\mathbf{N}^s$, $\mathbf{N}$, $\mathbf{K}^s$, $\mathbf{K}$, $\mathbf{G}^T$, $\mathbf{G}$ and $\mathbf{D}$ can be calculated with the following formulas:

$$M^S_{\alpha\beta} = \int_\Omega c^* S_a S_b \,\mathrm{d}\Omega \tag{13}$$

$$N^S_{\alpha\beta} = \int_\Omega \rho c S_a u_k S_{b,k} \,\mathrm{d}\Omega \tag{14}$$

$$K^S_{\alpha\beta} = \int_\Omega \lambda S_{a,j} S_{b,j} \,\mathrm{d}\Omega \tag{15}$$

$$M_{\alpha\beta} = \int_\Omega \rho c S_a S_b \, \mathrm{d}\Omega \tag{16}$$

$$K_{\alpha\beta} = \int_\Omega \mu S_{a,k} S_{b,k} \delta_{ij} \, \mathrm{d}\Omega + \int_\Omega \mu S_{a,j} S_{b,i} \, \mathrm{d}\Omega \tag{17}$$

$$N_{\alpha\beta} = \int_\Omega \rho S_a u_k S_{b,k} \delta_{ij} \, \mathrm{d}\Omega \tag{18}$$

$$G_\alpha = \int_\Omega S_{a,i} S_b \, \mathrm{d}\Omega \tag{19}$$

$$D_{\alpha\beta} = \int_\Omega \rho \mu \frac{f_l}{K_\varepsilon} S_a S_b \delta_{ij} \, \mathrm{d}\Omega \tag{20}$$

$$G_\beta^T = \int_\Omega S_{b,j} S_a \, \mathrm{d}\Omega \tag{22}$$

$$F_\alpha = \int_\Omega \rho S_a f_i \, \mathrm{d}\Omega, \tag{23}$$

where α, β are indices of single element matrix, a and b have the range up to number of nodes in an element, i, j, k have the range up to a number of dimensions, S is shape function of finite elements, and δ is Kronecker delta.

Equations in that form can be solved with carefully selected finite elements [8]. The approach which is described in this paper is based on the use of the stabilized Finite Element Method [9]. It makes it possible to avoid limits set by the Ladyzhenskaya-Babuska-Breezi condition.

Treating the drag force part in stabilization requires special care [10]. An approach used in this paper determines stabilization coefficient values by the velocity of the liquid and limits it proportionally to the volume of liquid fraction.

During the calculations the authors assumed a small time step, therefore the authors used temperature from the previous time step when temperature was needed to determine actual material properties values. That approach allows to treat solidification equation as linear and to solve it without Navier-Stokes equations, which makes for a better overall performance [11]. What is more, such an approach allows to use lumped mass matrix in solidification equation [11, 12]. At the moment any adaptive time stepping strategy was not implemented. A size of time step was only based on the authors' experience in computer simulations. Use an adaptation method could be planned in the future work.

Bearing these assumptions in mind and using theta scheme for time integration, the final form of equations solved in the model is:

$$[\mathbf{M}^s + \mathbf{M}^s_{SUPG} + \Delta t\theta(\mathbf{N}^s + \mathbf{N}^s_{SUPG} + \mathbf{K}^s)]\mathbf{T}^{t+1} = [\mathbf{M}^s + \mathbf{M}^s_{SUPG} + \Delta t(1-\theta)(\mathbf{N}^s + \mathbf{N}^s_{SUPG} + \mathbf{K}^s)]\mathbf{T}^t \tag{24}$$

$$\begin{aligned}&\big[\mathbf{M} + \mathbf{M}_{SUPG} + \\ &\Delta t\theta\big(\mathbf{N} + \mathbf{N}_{SUPG} + \mathbf{K} + \mathbf{D} + \mathbf{D}_{SUPG}\big)\big]\mathbf{u}^{t+1} - \Delta t\mathbf{G}\mathbf{p}^{t+1} + \\ &+\big[\mathbf{M} + \mathbf{M}_{SUPG} + \Delta t(1-\theta)\big(\mathbf{N} + \mathbf{N}_{SUPG} + \mathbf{K} \\ &\qquad + \mathbf{D} + \mathbf{D}_{SUPG}\big)\big]\mathbf{u}^t = \\ &= \Delta t\big[\theta\big(\mathbf{F} + \mathbf{F}_{SUPG}\big) + (1-\theta)\big(\mathbf{F} + \mathbf{F}_{SUPG}\big)\big]\end{aligned} \tag{25}$$

$$\begin{aligned}&\big[\mathbf{M}_{PSPG} + \Delta t\theta\big(\mathbf{G}^T + \mathbf{N}_{PSPG} + \mathbf{D}_{PSPG}\big)\big]\mathbf{u}^{t+1} - \\ &\Delta t\mathbf{G}_{PSPG}\mathbf{p}^{t+1} + \\ &+\big[\mathbf{M}_{PSPG} + \Delta t(1-\theta)\big(\mathbf{G}^T + \mathbf{N}_{PSPG} + \mathbf{D}_{PSPG}\big)\big]\mathbf{u}^t = \\ &= \Delta t[\theta\mathbf{F}_{PSPG} + (1-\theta)\mathbf{F}_{PSPG}],\end{aligned} \tag{26}$$

where matrices with *SUPG* (Streamline Upwind Petrov-Galerkin) and *PSPG* (Pressure Stabilized Petrov-Galerkin) are terms supplied by stabilization, Δt is time step, and θ is parameter determining a type of time integration scheme (0 for Euler Backward and 0.5 for Cranck-Nicolson).

While SUPG should repel oscillations in solutions that occur due to high velocities, obtaining a solution with oscillations (especially temperature) is still possible thanks to high gradients. To avoid oscillations caused by high gradients it is common to use a diagonal mass matrix in the heat transfer simulations.

$$\begin{bmatrix} \mathbf{M}^S_{11} & \mathbf{M}^S_{12} & \mathbf{M}^S_{13} \\ \mathbf{M}^S_{21} & \mathbf{M}^S_{22} & \mathbf{M}^S_{23} \\ \mathbf{M}^S_{31} & \mathbf{M}^S_{32} & \mathbf{M}^S_{33} \end{bmatrix} \Longrightarrow \cdots$$
$$\begin{bmatrix} \mathbf{M}^S_{11} + \mathbf{M}^S_{12} + \mathbf{M}^S_{13} & 0 & 0 \\ 0 & \mathbf{M}^S_{21} + \mathbf{M}^S_{22} + \mathbf{M}^S_{23} & 0 \\ 0 & 0 & \mathbf{M}^S_{31} + \mathbf{M}^S_{32} + \mathbf{M}^S_{33} \end{bmatrix} \tag{27}$$

One of the tasks, which the authors contemplated during their work, was a possibility of using the SUPG and the diagonal mass matrix in one model to find out how well they work together. This model uses Newton-Raphson approach for linearization of Navier-Stokes equations.

3. Simulations

The model described in section 2 was implemented by authors hereof in C++ language with the use of TalyFEM finite element routines library [13] and PETSc, as a provider of linear algebra algorithms and data structures [14].

The results of calculations taking into account convection are shown for the domain presented in Fig. 1. The boundary conditions utilised following parameters: Newton boundary condition on all sides of mould had the environment temperature equal to 300 K and heat exchange coefficient was equal to 10 W/(m K). Continuity condition assumed a value of 1000 W/(m K) for heat transfer through a separation layer.

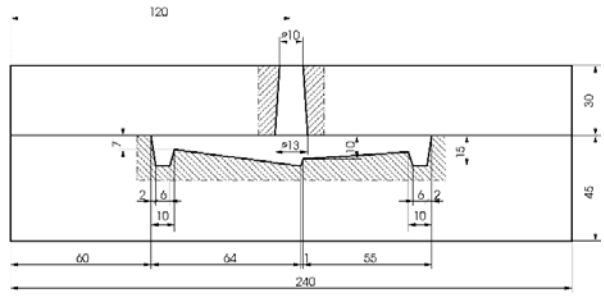

Fig. 1. View of the casting and mold with dimensions (in mm)

A summary of the material properties can be found below in Table 1 (for casting) and Table 2 (for mould). That properties correspond on a binary alloy Al-2%Cu.

Table 1.
Material properties for casting

Quantity name	Unit	Value
Density ρ_s	kg/m^3	2824
Density ρ_l	kg/m^3	2498
Specific heat c_s	J/(kg K)	1077
Specific heat c_l	J/(kg K)	1275
Thermal conductivity λ_s	W/(m K)	262
Thermal conductivity λ_l	W/(m K)	104
Solidus temperature T_s	K	853
Liquidus temperature T_l	K	926
Solidification temperature of pure component T_M	K	933
Eutectic temperature T_E	K	821
Heat of solidification L	J/kg	390000
Solute partition coefficient k	-	0.125
Viscosity μ	kg/(m s)	0.004
Expansion coefficient β	1/K	0.0001
Secondary dendrite arm spacing K_0	m	1.4*10^{-11}

Table 2.
Material properties for mould

Quantity name	Unit	Value
Density ρ_s	kg/m^3	7500
Specific heat c_s	J/(kg K)	620
Thermal conductivity λ_s	W/(m K)	40

The computational domain comprised 280344 nodes and 570708 triangle finite elements. Time step used in time integration was equal to 0.025 s and time integration used a value of θ equal to 1 (Euler Backward). Total run time for our simulation was 25 s. The results of the computer simulation are presented for the first 8 s because after that time there was only occurred cooling phenomenon.

Fig. 2 shows the results of the comparison. The effect of convection is not visible there, as curves for cases, with and without convection, overlap due to small volume of casting that prevented convection forces from achieving greater values.

Plots of velocity vectors of liquid metal are shown in Figs. 3 to 7. Figs. 6-7 show the movement of liquid metal almost stopped after 4 seconds. The maximum value of velocity was 0.003 m/s as shown in Fig. 5. The value of velocity appears not to be sufficient to make an impact on the temperature values.

Corresponding temperature and solid fraction maps are presented in Fig. 8 to 12 and Figs. 13 to 17, respectively. They are shown solely for a case with convection, as differences would be hard to notice between cases with and without convection. The results show that this casting solidifies fast. There are no places in the casting that are in a fully liquid state after 4 seconds. The minimal amount of solid fraction is equal to 0.66 after 8 seconds. This shape of casting was chosen because the authors have access to some experimental data that describes the solidification process in this case.

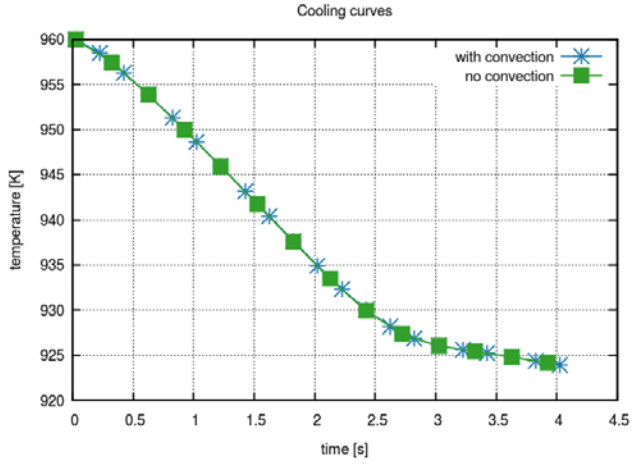

Fig. 2. Cooling curves of point that lies in centre of the casting.

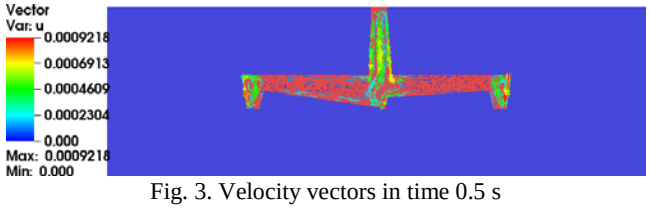

Fig. 3. Velocity vectors in time 0.5 s

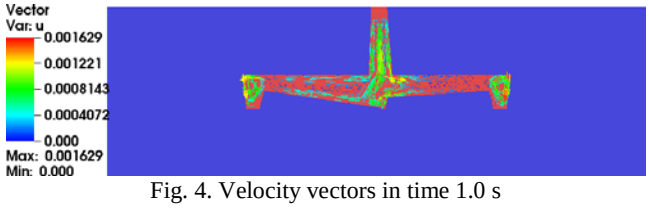

Fig. 4. Velocity vectors in time 1.0 s

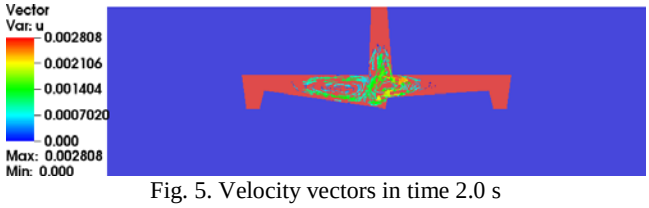

Fig. 5. Velocity vectors in time 2.0 s

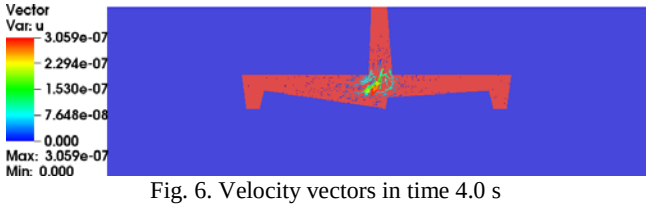

Fig. 6. Velocity vectors in time 4.0 s

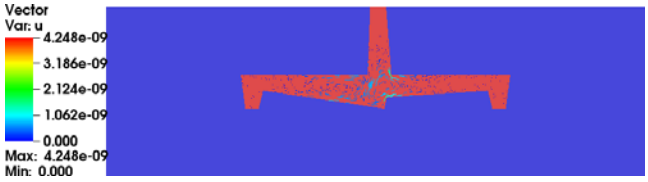

Fig. 7. Velocity vectors in time 8.0 s

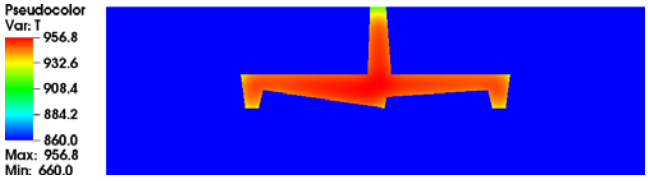

Fig. 8. Temperature after 0.5 s

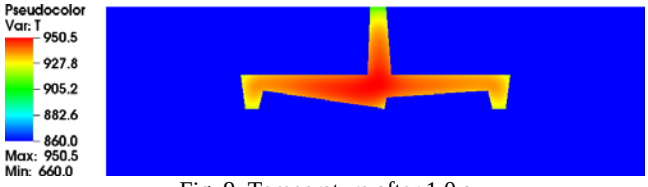

Fig. 9. Temperature after 1.0 s

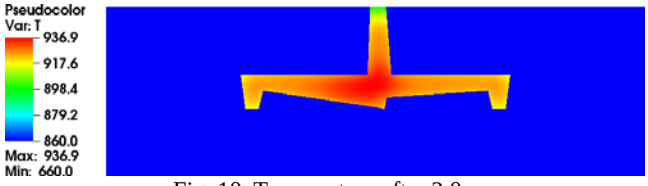

Fig. 10. Temperature after 2.0 s

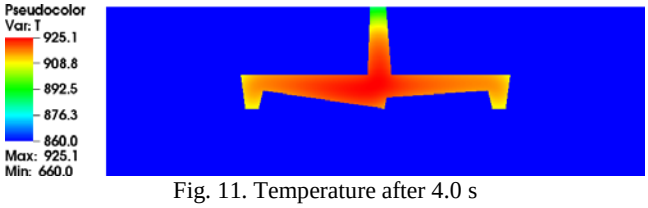

Fig. 11. Temperature after 4.0 s

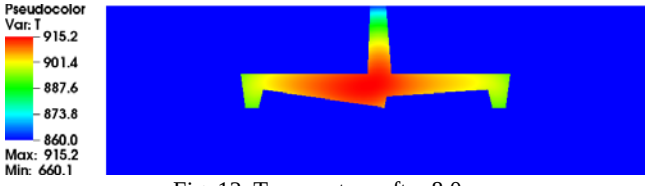

Fig. 12. Temperature after 8.0 s

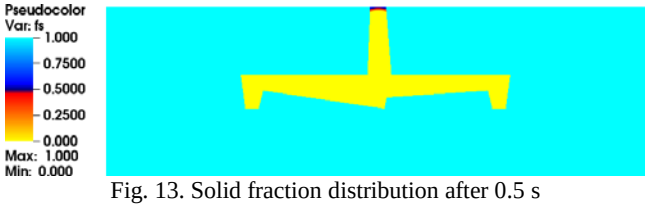

Fig. 13. Solid fraction distribution after 0.5 s

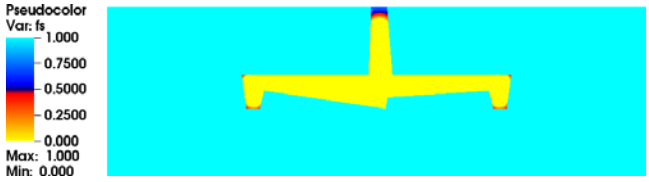

Fig. 14. Solid fraction distribution after 1.0 s

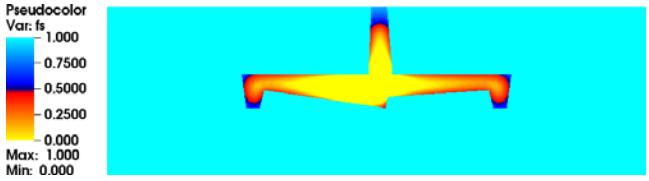

Fig. 15. Solid fraction distribution after 2.0 s

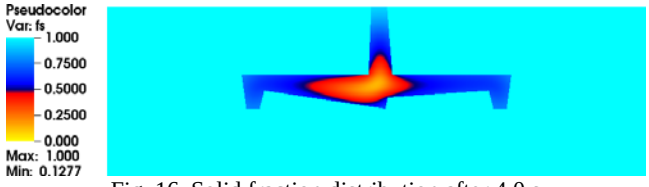

Fig. 16. Solid fraction distribution after 4.0 s

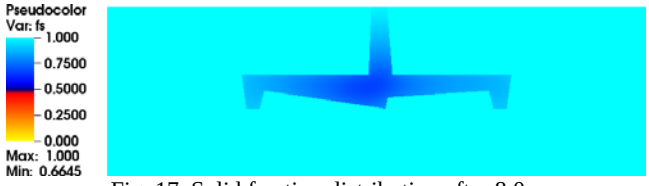

Fig. 17. Solid fraction distribution after 8.0 s

4. Summary

The paper discusses the problem of convection in solidification simulations. It shows the stages of the development of model and problems connected with the occurrence of momentum and continuity equations. Included computations show, that although small convection in the casting can affect results concerning the temperature and solid fraction maps, it is difficult to observe such phenomenon in this case because the cast is too small. However, the authors assume that it could be found in bigger casts (that issue was discussed for only simple shape in [15]), which will be the subject of their further simulations. Moreover, on the basis of calculations, the authors noticed that using diagonal mass matrix is extremely effective in the linear formulation, because oscillations in obtained results disappear almost completely (what was discussed in [11]). The main aims in the development of the tools for numerical computing are to make them i) fast, ii) cheap (simulations on workstations), iii) flexible (general purpose solver), iv) accurate (adaptive error control) [16]. The authors' software, which is still in development, satisfies all of these conditions.

Future work plans include an experimental comparison of results as the presented model has so far been checked only against benchmark problems.

References

[1] Bokota, A. & Iskierka, S. (1994). Finite element method for solving diffusion-convections problems in the presence of a moving heat point source. *Finite Elements in Analysis and Design*. 17(2), 89-99.

[2] Skrzypczak, A.T., Wegrzyn-Skrzypczak, E. & Winczek, J. (2015). Effect of natural convection on directional solidification of pure metal. *Archives of Metallurgy and Materials*. 60(2), 835-841.

[3] Stefanescu, D.M. (2002). *Science and Engineering of Casting Solidification*. New York: Kluwer Academic.

[4] Feng, W., Xu, Q. & Liu, B. (2002). Microstructure simulation of alluminium alloy using parallel computing technique. *ISIJ International*. 42(7). 702-707.

[5] Michalski, G., Sczygiol, N. (2014). Using CUDA architecture for the computer simulation of the casting solidification process. In Proceedings of the International MultiConference of Engineers and Computer Scientists 2014, IMECS 2014, March 12 - 14, 2014, Hong Kong. Vol II (pp. 933-937).

[6] Gawronska, E., Sczygiol, N. (2010). Application of mixed time partitioning methods to raise the efficiency of solidification modelling. In 12th International Symposium on Symbolic and Numeric Algorithms (SYNASC), Sep 23-26, 2010, Timisoara, Romania. (pp. 99-103).

[7] Bennon, W.D. & Incropera, F.P. (1987). A continuum model for momentum, heat and species transport in binary solid-liquid phase change systems - I. Model formulation. *International Journal of Heat and Mass Transfer*. 30(10), 2161-2170.

[8] Brezzi, F. (1974). On the existence, uniquess and approximation of saddle-point problems arising from lagrangian multipliers, *ESAIM: Mathematical Modelling and Numerical Analysis.* 8(R2). 129-151.

[9] Brooks, A.N., Hughes, T.J.R. (1990). Streamline Upwind/Petrov-Galerkin formulations for convection dominated flows with particular emphasis on the incompressible Navier-Stokes equations. *Computer Methods in Applied Mechanics and Engineering* – Special Edition on the 20th Anniversary. 199-259.

[10] Zabaras, N. & Samanta, D. (2004). A stabilized volume-averaging finite element method for flow in porous media and binary alloy solidification processes. *International Journal for Numerical Methods in Engineering*. 60(5). 1-38.

[11] Dyja, R., Gawronska, E. & Grosser, A. (2017). Numerical problems related to solving the Navier-Stokes equations in connection with the heat transfer with the use of FEM. *Procedia Engineering*. 177, 78-85.

[12] Zych, M. (2015). Effect of mass matrix forms on numerical simulation results in heat conduction modelling. *Journal of Applied Mathematics and Computational Mechanics.* 14(3), 149-156.

[13] Kodali, H.K. & Ganapathysubramanian, B. (2012). A computational framework to investigate charge transport in heterogeneous organic photovoltaic devices. *Computer Methods in Applied Mechanics and Engineering*. 247, 113-129.

[14] Balay, S., Gropp, W.D., McInnes, L.C. & Smith, B.F. (1997). Efficient Management of Parallelism in Object Oriented Numerical Software Libraries. *Modern Software Tools in Scientific Computing*. 163-202.

[15] Dyja, R., Gawrońska, E. & Grosser, A. (2018). A computer simulation of solidification taking into account the movement of the liquid phase. *MATEC Web of Conferences*. 157. 02008.

[16] Galdi, G.P., Heywood, J.G., Rannacher, R. (2000). *Fundamental directions in mathematical fluid mechanics.* Birkhäuser Verlag.